

Hans-Jakob Schindler <sup>1</sup>

## On the Significance of Crack Tip Shielding in Fatigue Threshold - Theoretical Relations and Experimental Implications

---

**Reference:** Schindler, H. J., " On the Significance of Crack Tip Shielding in Fatigue Threshold - Theoretical Relations and Experimental Implications," *Fatigue Crack Growth Thresholds, Endurance Limits, and Design*, ASTM STP 1372, J. C. Newman and R. S. Piascik, Eds., American Society for Testing and Materials, West Conshohocken, PA, 1999.

**Abstract:** The fatigue crack growth (FCG) threshold behavior of elastic-plastic materials is analyzed theoretically by simplistic mechanical considerations. Emphasis was laid upon two of the key aspects of threshold, which are both still controversially discussed in the literature: intrinsic threshold and extrinsic crack tip shielding. The analytical relations derived from the model confirm experimental indications, that at R-ratios beyond a certain limit FCG and its threshold is governed by intrinsic mechanisms, whereas at lower R it is crucially influenced by extrinsic shielding mechanisms. The latter are postulated to consist of a crack-closure and a non-closure part, which is confirmed by preliminary experimental data as well as data from the literature. To measure crack closure independently, a new experimental technique, the so-called cut compliance method, is proposed, which is shown by some preliminary tests to work well even in the threshold regime. The model and the derived mathematical relations also enable one to distinguish between those parts of the threshold that are inherently associated with FCG, and the ones that are geometry- or load-history-dependent. Therewith conservatively transferable threshold data can be obtained.

**Keywords:** crack tip shielding, crack closure, intrinsic threshold, experimental, residual stress, influence functions, cut compliance method, threshold chart, R-effect

### Nomenclature

a	crack length and cut length, respectively
$a_n, a_f$	depth of initial notch and final length of fatigue crack, respectively
C	constant in the crack-growth equation
$C_{op/pl}$	$= K_{op/pl} / K_{max}$
CC	cut compliance (-method)
$\Delta K$	SIF range, $\Delta K = K_{max} - K_{min}$

---

<sup>1</sup> Senior research engineer, Swiss Federal Labs. for Materials Testing and Research (EMPA), CH-8600 Dübendorf, Switzerland.

$\Delta K_{\text{eff}}$	range of SIF that produces plastic strains in the vicinity of the crack-tip
$\Delta K_{\text{th}}$	value of $\Delta K$ below which no FCG occurs
$\Delta K_{\text{th/int}}$	intrinsic component of $\Delta K_{\text{th}}$
$\varepsilon_M$	strain at measurement point M
FCG	fatigue crack growth
$K_i$	SIF at initiation of ductile tearing
$K_{\text{Irs}}$	SIF due to residual stresses or crack closure stresses
$K_{\text{max/th}}$	threshold value of $K_{\text{max}}$ for low R
$K_{\text{min}}, K_{\text{max}}$	minimum and maximum SIF of a load cycle, respectively
$K_{\text{nc}}$	extrinsic shielding of the crack tip other than crack closure, in terms of SIF
$K_{\text{op}}$	SIF required to overcome the contact stresses acting between the crack faces
$K_{\text{op/pl}}$	plasticity induced crack closure SIF
$K_{\text{op/ext}}$	SIF due to crack closure remote from the crack tip
$K_{\text{sh}}$	extrinsic shielding of the crack tip loading in terms of SIF
n	exponent in the crack-growth equation
R	load or SIF ratio, $R=K_{\text{min}}/K_{\text{max}}$
$R_{\text{op}}$	$R_{\text{op}}=K_{\text{op}}/K_{\text{max}}$
$R_p, R_m$	yield stress and ultimate tensile strength, resp.
$R_{\text{sh}}$	value of R at the transition between shielded and non-shielded crack tip
SIF	stress intensity factor
Z	influence function

The existence of a threshold of the stress intensity range,  $\Delta K_{\text{th}}$ , below which no crack propagation occurs, was postulated shortly after fracture mechanics parameters were first used to correlate the rates of fatigue crack growth (FCG) [1]. Enabling safe life calculations to be simplified, fatigue tests to be shortened, and giving some theoretical support to the widely used concept of fatigue strength and endurance limits, the FCG-threshold plays an important role in engineering fatigue. However, most of the knowledge about this phenomenon is of empirical nature, and the underlying mechanisms are far from being satisfactorily understood. The FCG-threshold is known to be affected by several parameters, like the R-ratio, stress history, environment, frequency, crack length, and geometry of the specimen or structural component [2]. So it is no surprise that there is a pronounced scatter in the experimental data reported in the literature [3]. Since threshold concepts applied in safe life calculations of structural components only make sense if there is no doubt that the data used are conservative, relatively high safety margins have to be applied when using experimental data in practical applications.

Regarding the number of influencing factors on the one hand and the experimental effort and costs to determine reliable threshold data according to ASTM E647 on the other, a mainly empirical approach to account for the threshold behavior in safe life predictions is not adequate. Neither is a purely theoretical one, since the physical processes involved are much too complex to be treatable purely theoretically. Thus, as in other fields of fracture mechanics, the most efficient way to come to quantitative predictions appears to be a semi-empirical one, which means using simplistic mechanical models in combination

with experimental data to determine the inevitable open parameters of the model. Whilst it should be general and flexible enough to reproduce the major experimental features and phenomena of the process, it also has to be simple enough to be analytically solvable. The above mentioned open constants should be as few as possible, physically well defined and experimentally easily measurable. However, at least as important as choosing an appropriate model is using it consistently in the evaluation of test data and in the FCG-prediction of a given structural component.

A key factor in FCG and threshold is crack closure [4-8]. Although this phenomenon has been known for more than two decades now and is in principle generally accepted as a typical feature of FCG, there still is no consensus about its physical relevance, its magnitude, its experimental and computational determination and the definition of characteristic parameters [9-13]. A variety of models and empirical formulas have been proposed in the literature to quantify this effect. The controversy especially concerns the threshold regime, where plane strain conditions prevail and the plasticity induced crack closure is relatively small. Another important question is the transferability of threshold values measured on a test specimen to structural components of other shapes and sizes. In the present paper some of these questions are tried to be further clarified by simplistic models and considerations. They allow to sort out transferable and non-transferable components of the threshold.

Probably one of the main reasons why a common view on this subject has not yet been achieved in the scientific community are the difficulties encountered when quantifying crack closure experimentally, since the usually applied compliance methods become inaccurate at low load ranges. In the present paper a new method, the cut compliance method, is proposed. The preliminary experimental results show the applicability of this method even in the threshold regime. The data obtained give additional information about the physical processes involved in the threshold behavior and allows one to distinguish between those components of the FCG-threshold, which are affected by the test specimen geometry and the testing conditions and those, which are inherently connected with the fatigue process. This differentiation is essential when dealing with the question of the transferability of the threshold data from the test specimen to a structural component.

## **Fatigue Crack Growth Law**

FCG results from local damage due to the repetitive plastic strains in the vicinity of the crack tip that result from a cyclic stress intensity factor (SIF) [3,4,14]. The latter, called the effective SIF-range  $\Delta K_{\text{eff}}$ , is formed by the external load reduced by the local crack-tip shielding effects like crack closure [5, 6]. It is an experimental fact, that there is a threshold of the effective SIF-range,  $\Delta K_{\text{th/int}}$ , where the crack ceases to grow. A suitable modification of Paris' law to account for this behavior is

$$\frac{da}{dN} = C \cdot ( \mathbf{DK}_{\text{eff}}^n - \mathbf{DK}_{\text{th/int}}^n ) \quad (1)$$

$\Delta K_{\text{th/int}}$  results from mechanisms that prevent micro-plastic effects to occur in the vicinity of the crack tip, like dislocations caught at grain boundaries, slip bands interrupted by

inclusions, microscopically finite crack tip radii, etc., so it is called the intrinsic FCG-threshold.  $\Delta K_{th/int}$  is considered to be a material property. Nevertheless it can be affected by factors like the environment and the loading frequency. The mathematical form of (1) assures that  $\Delta K_{th/int}$  has the awaited minor effect on the FCG-rate  $da/dN$  at higher SIF-ranges.

$\Delta K_{eff}$  is generally given by

$$\Delta K_{eff} = \begin{cases} K_{max} - K_{sh} & \text{for } R < R_{sh} \\ \Delta K & \text{for } R > R_{sh} \end{cases} \quad (2)$$

where

$$R = \frac{K_{min}}{K_{max}} = 1 - \frac{\Delta K}{K_{max}} \quad (3)$$

$$R_{sh} = K_{sh}/K_{max} \quad (4)$$

$K_{sh}$  represents the total extrinsic shielding in terms of SIF, the term "extrinsic" meaning due to secondary mechanical forces acting at or near the crack surfaces [12, 15], such as the well known crack closure  $K_{op}$ . However, directly measured crack closure values  $K_{op}$  often are significantly lower than the ones determined indirectly by crack growth observation [11, 17], which implies that crack closure might be not the only shielding effect of a fatigue crack tip in the threshold regime. Therefore, we assume  $K_{sh}$  to be composed of crack-closure  $K_{op}$  and an additional component,  $K_{nc}$ , i.e.

$$K_{sh} = K_{op} + K_{nc} \quad (5)$$

Since extrinsic shielding of other type than crack closure is hardly possible in a 2D-system,  $K_{nc}$  is likely to be associated with 3D-effects such as the crack curvature, which in general deviates from a straight line, and local non-planar crack-growth caused by microstructural features, leading to crack surface roughness. Regarding the former and the particularly local nature of closure effects at small load ranges (where a substantial part of the closure SIF is formed by contact stresses within a few tenths of a millimeter behind the crack-tip), it is obvious that closure effects can not be completely captured by the usual 2D-considerations. The latter results in local friction, Mode-II- and Mode-III effects that can contribute to crack-tip shielding but not to crack closure as measured by direct 2D-methods such as ASTM E 647 or the CC-method discussed later on. According to these considerations,  $K_{nc}$  is likely to depend on the micro-structure of the material and the specimen or component thickness.

Concerning  $K_{op}$ , it is suitable to distinguish between two components,

$$K_{op} = K_{op/pl} + K_{op/ext} \quad (6)$$

The first,  $K_{op/pl}$ , represents the closure-SIF due to the inevitable local plastic deformation at the crack tip. The second,  $K_{op/ext}$ , results from additional closure effects such as corrosion products stuck to the crack faces, asperities and roughness of the crack surface, including plasticity-induced closure of the crack-faces remote from the crack-tip, due to

overloads at earlier stages of the crack. Thus,  $K_{op/pl}$  can be considered to be inherently associated with FCG in elastic-plastic materials, whereas  $K_{op/ext}$  depends on system-specific conditions.

An analytical or a Finite-Element model is required to split  $K_{op}$  according to (6). In [4],  $K_{op/pl}$  was calculated by means of a strip yield model from the condition that closure-free crack-growth requires the slope of the crack contour at the physical crack tip to be zero, which led to

$$K_{op/pl} = C_{op/pl} K_{max} \quad (7)$$

with

$$C_{op/pl} \cong \frac{R_p}{R_p + R_m} \quad \text{for plane stress} \quad (8)$$

where  $R_p$  and  $R_m$  denote the yield strength and the ultimate tensile strength, respectively. Physically,  $C_{op/pl}$  represents the ratio of a representative flow stress in tension to the one for subsequent compression. The approximation (8) holds for plane stress. In plane strain, which often prevails in the threshold regime, the strip yield model as used in [4] is less accurate. Due to triaxiality, the local flow stress is increased, the strain correspondingly decreased, and the ratio of tensile to compressive flow stress is lower [16], resulting in a considerably reduced crack closure [7]. Following roughly pattern of the derivation in [4] and regarding the results of [16], we account for these effects roughly by replacing in (8)  $R_m$  by  $2R_m$ , thus

$$C_{op/pl} \cong \frac{R_p}{R_p + 2R_m} \quad \text{for plane strain} \quad (9)$$

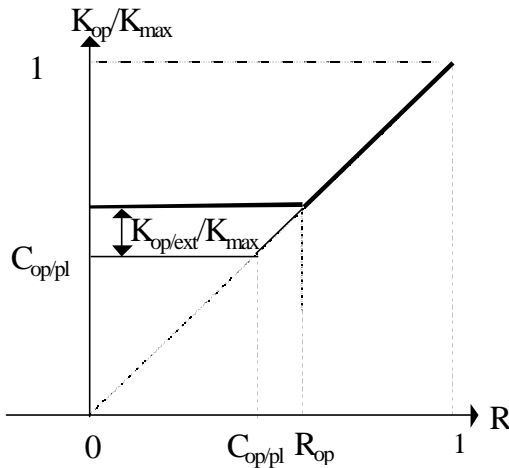


Fig. 1 - General behavior of the opening SIF as a function of  $R$  according to the present model

The general behavior of  $K_{op}$  as given by (6) - (9) is shown in Fig. 1 as a function of  $R$  which is in good agreement with empirical and numerical behavior [5-8]. In Fig. 2,  $K_{op}$  is shown as a function of  $K_{max}$  which also is in qualitative agreement with the behavior of experimental data [8]. Fig. 2 also shows a possible way to estimate  $C_{op/pl}$  experimentally.

Actually, as shown in [13, 16],  $K_{op/pl}$  depends not only on  $K_{max}$  as stated by (6a-6c), but, at least to some degree, also on  $K_{min}$ , since low or negative values of  $K_{min}$  tend to reduce the closure effect by additional plastic compression of the crack surface. This effect is disregarded here for the sake of simplicity (see [18] for further discussion).

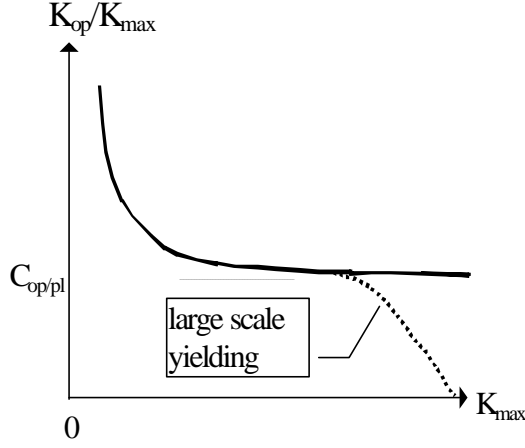


Fig. 2 - General behavior of  $K_{op}$  as a function of  $K_{max}$  for  $R < R_{sh}$

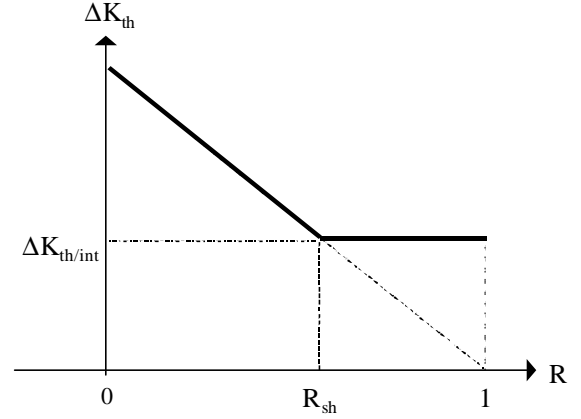


Fig. 3 - Dependence of  $K_{th}$  on  $R$ .

With (5) - (9), (2) becomes

$$\Delta K_{eff} = \begin{cases} (1 - C_{op/pl}) \cdot K_{max} - K_{op/ext} - K_{nc} & \text{for } R < R_{sh} \\ \Delta K & \text{for } R > R_{sh} \end{cases} \quad (10)$$

where

$$R_{sh} = (K_{op} + K_{nc})/K_{max} \quad (11)$$

### Threshold Behavior

The FCG-threshold in terms of  $\Delta K$ ,  $\Delta K_{th}$ , is obtained by inserting (10) and (11) in (1) and setting  $da/dN=0$ . One obtains

$$\Delta K_{th} = \Delta K_{th0} \cdot (1 - R) \quad \text{for } R < R_{sh} \quad (12a)$$

$$\Delta K_{th} = \Delta K_{th/int} \quad \text{for } R > R_{sh} \quad (12b)$$

where

$$\Delta K_{th0} = \frac{\Delta K_{th/int} + K_{op/ext} + K_{nc}}{1 - C_{op/pl}} \quad (13)$$

$\Delta K_{th}$  as given by (12a) and (12b) is shown in Fig. 3. It compares well with experimental data (see Fig. 7 below and e.g. [12, 17, 19]), indicating that the model used here is able to

reproduce the main characteristics of the FCG and the corresponding threshold. Inserting (3) in (12) and (13) leads to

$$K_{\max/th} = \frac{\Delta K_{th/int} + K_{op/ext} + K_{nc}}{1 - C_{op/pl}} \quad \text{for } R < R_{sh} \quad (14a)$$

$$DK_{th} = DK_{th/int} \quad \text{for } R > R_{sh} \quad (14b)$$

The conditions for non-propagation corresponding to (14a) and (14b), i.e.  $K_{\max} < K_{\max/th}$  for  $R < R_{sh}$  and  $\Delta K < \Delta K_{th}$  for  $R > R_{sh}$ , respectively, form the shaded area in the  $K_{\max}$ -vs.- $\Delta K$ -plane (Fig. 4), confirming experimental and theoretical findings of other authors [15, 16, 17, 19]. This area, called in the following the threshold-chart, characterizes the threshold behavior of a certain test specimen or component. It is defined by only two parameters,  $\Delta K_{th/int}$  and  $K_{\max/th}$ . Correspondingly, only two threshold tests are required to establish the threshold chart: One at  $R < R_{sh}$ , e.g.  $R=0.1$ , to deliver  $K_{\max/th}$ , the other at  $R > R_{sh}$ , e.g.  $R=0.7$ ,

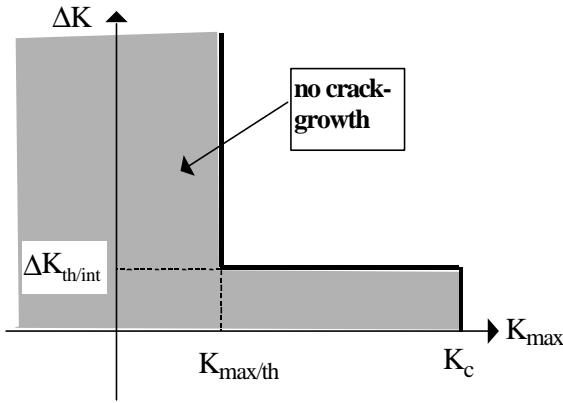


Fig. 4 - Conditions for no crack propagation in the test specimen ("threshold chart").

to deliver  $\Delta K_{th/int}$ . By performing first the former at a constant (low)  $R$ -value, and then - using the same specimen - the other at a constant  $K_{\max}$  (as described in [11], with  $K_{\max}$  chosen to be about the mean value of  $K_{Ic}$  and  $K_{\max}$  of the previous test), the complete threshold chart can in principle be obtained from just one single specimen.

Of course, neither  $K_{\max}$  nor  $\Delta K$  are unbounded, but limited by additional conditions of fracture mechanics and strength of materials. For example,  $K_{\max}$  is obviously limited to  $K_{\max} < K_c$ , or, in case of stress corrosion cracking or creep, to  $K_{\max} < K_{Isc}$  or  $K_{\max} < K_{creep}$ , respectively (Fig. 4). Similar limits are

imposed on the  $\Delta K$ -values by the condition of general yielding under compression. The corresponding upper and left-hand boundary of the shaded area, which turns out to be system- and crack-length-dependent [18], is not further considered here.

From (3) and (14a, b) one obtains an equation to determine  $R_{sh}$  or  $K_{sh}$ , respectively, from experimentally determined  $\Delta K_{th/int}$  and  $K_{\max/th}$  i.e.

$$R_{sh} = \frac{K_{sh}}{K_{\max/th}} = 1 - \frac{\Delta K_{th/int}}{K_{\max/th}} \quad (15)$$

According to (11),  $R_{sh}$  represents an upper bound of  $R_{op} = K_{op}/K_{\max}$ , thus

$$K_{op} \leq R_{sh} \cdot K_{\max} \quad (16)$$

## Lower-Bound FCG-Thresholds

The relations (12a, b) and (14a, b), respectively, exhibit the various ingredients of the FCG-threshold. According to their definition and the discussion above, only  $\Delta K_{th/int}$  is a "pure" material property (though affected by additional factors like loading frequency and environment).  $C_{op/pl}$  is process- and thickness-dependent.  $K_{op/ext}$  depends definitely at least on the crack- and specimen-geometry, the environment and the load-history.  $K_{nc}$  is expected to depend on the thickness of the specimen or component, respectively, increasing with increasing thickness. Thus, for a structural component of the same thickness as the specimen, a lower bound of  $K_{max/th}$ , which can be conservatively used to predict the fatigue behavior of a structure, is obtained by setting  $K_{nc}$  and  $K_{op/ext}$  equal to zero in (13) or (14a), i.e.

$$\Delta K_{max/th/min} = \frac{\Delta K_{th/int} + K_{nc}}{1 - C_{op/pl}} \quad (17)$$

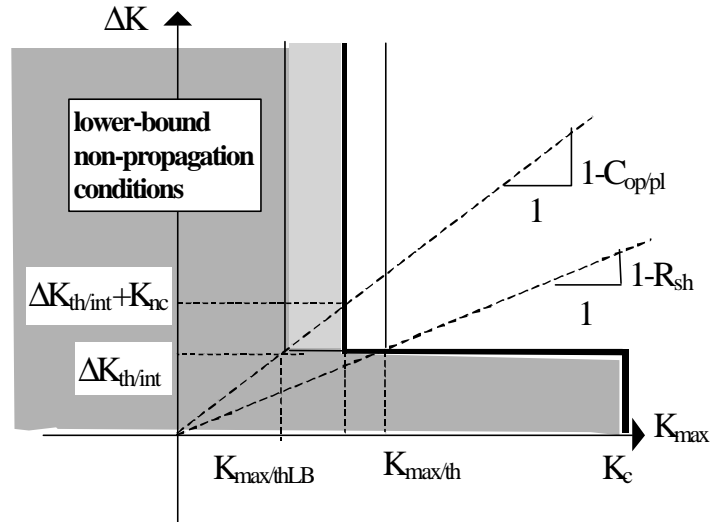


Fig. 5 - Lower-bound- threshold chart and its relation to the chart of non-propagation in the specimen (Fig. 4). The dark-shaded area represents its conservative part ( $K_{nc} = 0$ ).

A lower bound of  $K_{max/th}$ , which can be used as a conservative threshold for any component- and crack-geometry, is obtained by neglecting  $K_{nc}$  as well and using the plane strain approximation of  $C_{op/pl}$ , thus

$$K_{max/th/LB} = \frac{\Delta K_{th/int} \cdot (R_p + 2R_m)}{2R_m} \quad (18)$$

The graphical representation of the conservative threshold charts according to (17) and (18) as well as the graphical determination of  $R_{sh}$  is shown in Fig. 5.

In order to determine  $K_{\max/th/\min}$  according to (17),  $K_{nc}$  is required. By (5) and (15), it is found to be

$$K_{nc} = K_{\max/th} - DK_{th/int} - K_{op} \quad (\text{for } R < R_{sh}) \quad (19)$$

where  $K_{op}$  has to be measured. For this purpose the cut compliance method is proposed in the next section.

### Measurement of $K_{op}$ by the Cut-Compliance Method

The cut compliance (CC-) method was primarily developed to measure residual stresses [19]. Its idea is to release the latter by introducing a cut into the considered body. From the strain change at a suitably chosen point M due to progressive cutting it is

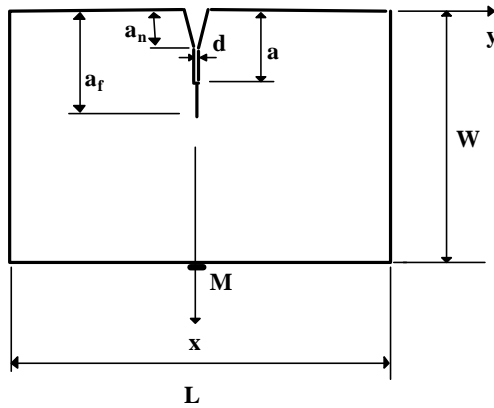


Fig. 6 - A cut of length  $a$  introduced in the plane of the fatigue crack of length  $a_f$ .

The actual length of the cut is denoted by  $a$ , its width by  $d$ . As derived in [21] the SIF at the tip of the cut due to the residual stresses is obtained from the strain  $\epsilon_M(a)$  measured at M by

$$K_{rs}(a) = \frac{E'}{Z(a)} \frac{d\epsilon_M}{da} \quad (20)$$

where  $E'$  denotes the generalized Young's modulus ( $E' = E$  for plane stress and  $E' = E/(1-\nu^2)$  for plane strain) and  $Z(a)$  the so-called influence function [21]. The latter is a unique function that depends on the component geometry, on the cut plane and on the location of the strain gage, but not on the residual stress distribution. For a relatively deeply cracked rectangular plate ( $a > W/4$ ,  $L > 2W$ ) (see Fig. 6), there is a simple exact solution for  $Z$  [22, 23]:

$$Z(a) = -\frac{7.952}{p \cdot (W - a)^{3/2}} \quad (21)$$

possible to calculate the distribution of the released stresses. Since fracture mechanics principles are used to establish the corresponding mathematical relations, the stress intensity factor due to residual stresses is delivered as well [21]. As shown in [22] it also enables the residual stresses in front of the crack-tip as well as the corresponding SIF to be measured in a rather simple way.

Briefly, the CC-method applied to crack closure measurements works as follows: A cut is progressively introduced along the plane of the fatigue crack. As an example, Fig. 6 shows the case of a rectangular plate containing a fatigue crack of a length  $a_f$ , which was initiated at the tip of a notch of length  $a_n$ .

The strain  $\varepsilon_M(a)$  is suitably measured by strain gages and recorded as a function of the cut depth  $a$ . Then, this curve has to be processed according to (20) and (21), which can be done by means of a simple spreadsheet computation. For  $a \geq a_f$  this gives the SIF due to closure stresses acting on the crack faces and the residual stresses in the ligament. At  $a = a_f$  equation (20) represents the required quantity  $K_{op}$ ,

$$K_{op} = K_{Irs}(a=a_f) \quad (22)$$

(Note that in the range  $a < a_f$ ,  $K_{Irs}(a)$  as delivered by (20) represents not the contact stresses acting on the crack-faces, but an upper bound thereof.) In cases of small cyclic loads like near the FCG-threshold, the compressive plastic zone is rather small and may probably neglected in most cases. Thus, the maximum (negative) value of  $K_{Irs}$  obtained by (20) from specimens loaded near the FCG-threshold represents an upper bound for  $K_{op}$ , which can be considered to be a good approximation of the actual  $K_{op}$ . Thus we assume

$$K_{op} \cong \max(|K_{Irs}|) \quad (23)$$

### Preliminary Experimental Results

To demonstrate the applicability of the CC-method and to give some examples of obtained closure and threshold data, the results of some tests performed within a feasibility-study [24] are given in the following. Four single edge notch specimens (Fig. 6;  $W=14$  mm,  $L=55$ mm and thickness  $B=10$ mm) of a structural steel of the type FeE460 ( $R_p=420$ N/mm<sup>2</sup>,  $R_m=550$ N/mm<sup>2</sup>) were loaded under cyclic pure bending. To obtain near-threshold data they were fatigued at constant R-values ( $R=0.1, 0.3, 0.5$  and  $0.7$ ) and a frequency of about 230 Hz by decreasing load range  $\Delta K$  until the growth rate was less than about  $10^{-7}$ mm/cycle. The measured near-threshold data are shown in Table 1 and in Fig. 7 as a function of R, and in the  $K_{max/th}$ -vs.- $\Delta K_{th}$ -plane, confirming the theoretical behavior of the model as shown in Fig. 1 and 3, respectively.

From the data in Table 1, the following characteristic threshold values are obtained:

$$\Delta K_{th/int} = 132 \text{ N/mm}^{3/2}, \quad K_{max/th} = 309 \text{ N/mm}^{3/2}, \quad (24a)$$

which results with (15) and (18) in

$$R_{sh} = 0.573, \quad K_{max/th/LB} = 182 \text{ N/mm}^{3/2} \quad (24b)$$

For the tensile properties given above, (7) and (9) deliver the local plasticity-induced crack closure  $K_{op/pl}$  in plane strain (which prevails in the present case) to be

$$K_{op/pl} = 0.276 \cdot K_{max} \quad (25)$$

To measure  $K_{op}$  by the CC-method the fatigued specimens were cut in two halves of  $W = 14$  mm and  $B = 4.9$ mm thickness resulted, in order to obtain two more or less

identically fatigued specimens. One of them was used to measure crack closure by the CC-method, and the other to measure the actual length of the fatigue crack. The cuts required for the CC-method were introduced by electric discharge machining (EDM). A typical strain signal as a function of the cut depth is shown in Fig. 8. To handle the noise that is typical for EDM-cutting,  $\varepsilon_M(a)$  was fitted to a polynomial of 6<sup>th</sup> order before (20) was applied, so the corresponding derivative could be taken analytically. The SIF obtained by using (20) and (21) on these polynomials are shown in Fig. 9. As expected, the maximum (actually minimum, since they are always negative) values of  $K_{Irs}$ , which are considered to be  $K_{op}$ , are located quite close to  $a=a_f$  (see Table 2 for  $a_f$ ), which confirms the assumption that led to (23).

Table 1 - Results of fatigue tests in the threshold regime

Specimen	L1	L2	L3	L4
R	0.1	0.3	0.5	0.7
$\Delta K_{th}$ [N/mm <sup>3/2</sup> ]	274	226	153	132
$K_{max/th}$ [N/mm <sup>3/2</sup> ]	305	315	307	440
$K_{sh}$ [N/mm <sup>3/2</sup> ] <sup>1)</sup>	173	183	175	-

<sup>1)</sup> determined by (15)

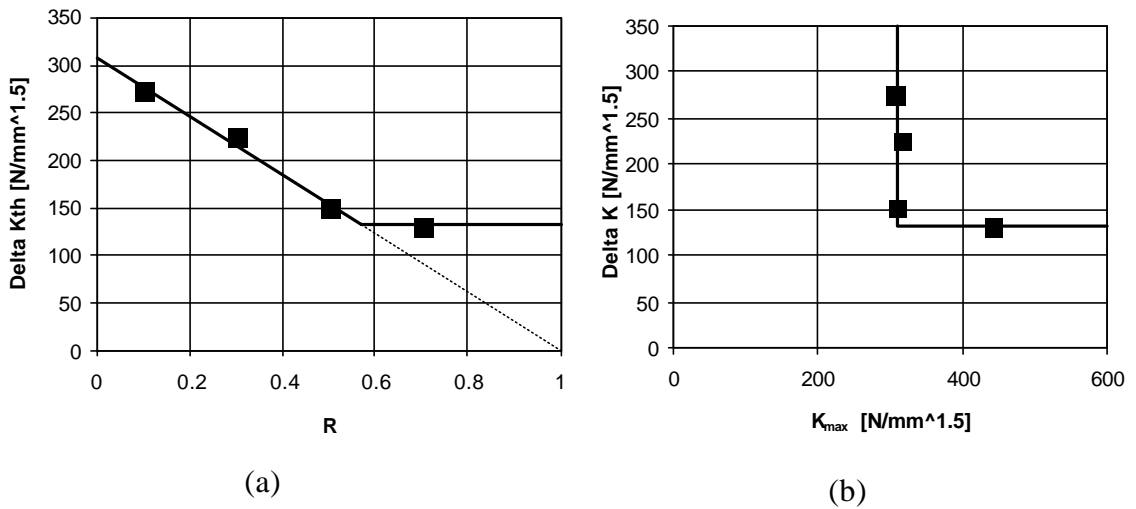


Fig. 7 - Experimental threshold values as a function of  $R$  (a) and  $K_{max}$  (b) in comparison with the behavior of the theoretical model (full lines).

After crack-length measurement the second halves of the described twin-specimens were used to determine  $K_{op}$  in the same way, but by mechanical sawing instead of EDM. As expected, the noise in the strain signal was considerably lower [24]. Qualitatively, the results were the same as the ones shown in Fig. 9. However, as shown in Table 2, there were considerable differences between the measured  $K_{op}$  of the twins, indicating that the fatigue process was not perfectly symmetrical.

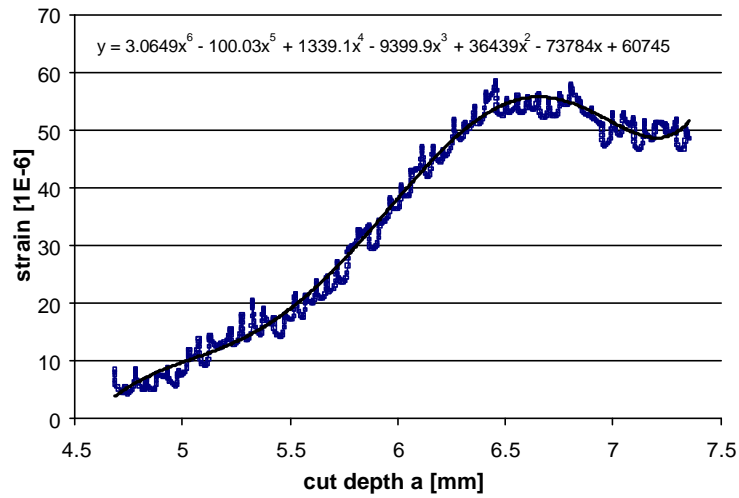


Fig. 8 - Measured strain  $\epsilon_M$  at the rear surface of specimen L2 as a function of cut depth, and the corresponding fitting polynomial

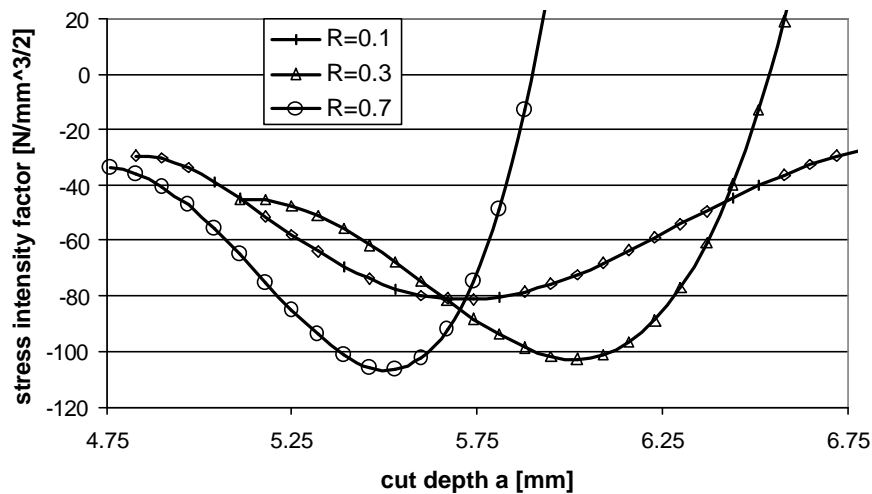


Fig. 9 - Measured stress intensity factor due to closure stresses and residual stresses as a function of cut depth

These preliminary experimental results show that  $K_{op}$  can be indeed significantly smaller than  $K_{sh}$ , indicating that there is a considerable amount of non-closure shielding. The analytically calculated  $K_{op/pl}$  are relatively close to the measured  $K_{op}$  in both cases, which means that either  $K_{op/ext}$  is relatively small in the present specimens, or that (7) and (9) give somewhat too high predictions.

Table 2 - Experimental data obtained from the CC-Method

Specimen	L1	L2	L3	L4
----------	----	----	----	----

R	0.1	0.3	0.5	0.7
$a_f$ [mm]	5.9	6.1	5.9	5.5
$K_{op}$ [ $N/mm^{3/2}$ ] <sup>1)</sup>	81/139	103/119	- <sup>2)</sup>	107/223

<sup>1)</sup> values for twin-specimens, determined according to (23); <sup>2)</sup> measurement failed because of a disconnection;

Table 3 - Experimental crack shielding parameters for  $R < R_{sh}$  (specimen L1 and L2)

Specimen	$K_{sh}$ <sup>1)</sup> [ $N/mm^{1.5}$ ]	$K_{op}$ <sup>2)</sup> [ $N/mm^{1.5}$ ]	$K_{nc}$ <sup>3)</sup> [ $N/mm^{1.5}$ ]	$K_{op/pl}$ <sup>4)</sup> [ $N/mm^{1.5}$ ]	$K_{op/ext}$ <sup>5)</sup> [ $N/mm^{1.5}$ ]	$K_{max/th/min}$ <sup>6)</sup> [ $N/mm^{1.5}$ ]
L1	173	110	63	84	26	269
L2	183	111	72	87	24	282

<sup>1)</sup> determined by (15); <sup>2)</sup> see Table 2(mean values); <sup>3)</sup> by (19); <sup>4)</sup> by (26); <sup>5)</sup> by (5); <sup>6)</sup> by (17) and (19)

## Discussion and Conclusions

The mechanics of FCG in the threshold regime are analyzed by means of a simplistic analytical model. It is shown that the conditions for non-propagation of a crack in a test specimen or a structural component is essentially characterized by two parameters,  $K_{max/th}$  and  $K_{th/int}$ . To determine these two parameters, basically two threshold tests are required: The first one is suitably performed at a low and constant R-ratio, and the second at a constant  $K_{max}$  which has to be considerably higher than  $K_{max}$  of the first test. Both these measurements can be performed on the same specimen.

Only one of these two threshold parameters,  $K_{th/int}$ , represents an independent material property. The other one,  $K_{max/th}$ , consists of several intrinsic and extrinsic components. With respect to their transferability, three types of contributions to  $K_{max/th}$  can be distinguished: intrinsic (material-dependent), inherent (material- and process-dependent), and system-dependent ones, as schematically shown in Fig. 10. These various contributions to the threshold explain why there often is a significant scatter in experimental threshold data reported in the literature. When applied to predict the behavior of a crack in a structural component, only the intrinsic and the process-inherent components should be taken into account. The present model offers the possibility to sort out these components and, therewith, to determine conservative lower bound thresholds from a few experimental results, in principle just from one threshold test at a high R-ratio. It is up to further experimental investigations to explore the accuracy and conservatism of this approach.

To fill the often observed gap between the effective stress range obtained by direct  $K_{op}$  - measurements and the one obtained indirectly from crack-growth measurements a so-called "non-closure" shielding was introduced. Its physical nature and influencing factors need further investigation. The preliminary experimental results indicate that the

introduced "non-closure" shielding effect  $K_{nc}$  is of relevant size in the threshold regime, about one third of the total extrinsic shielding. The physical origin of  $K_{nc}$  is not quite clear yet. It seems to be mainly due to local closure, crack front curvature and other 3D-effects that can not be captured with a 2D-consideration of crack closure. Correspondingly,  $K_{nc}$  is expected to increase with increasing specimen thickness. Whereas crack closure is higher in plane stress than in plane strain, the non-closure shielding is likely to behave in the opposite way. Thus, these two effects tend to compensate each other.

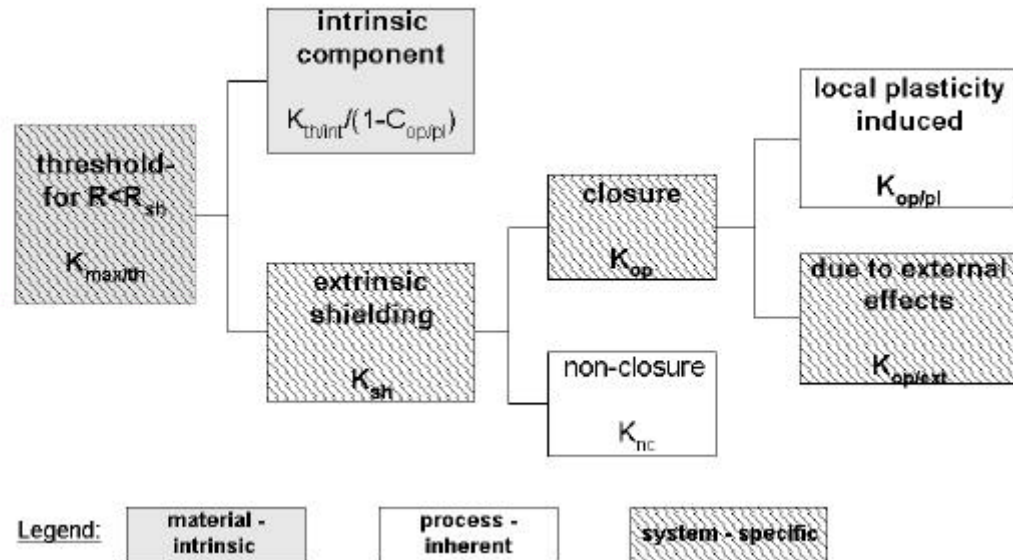


Fig. 10 - Composition of the threshold parameter for  $R < R_{sh}$ ,  $K_{max/th}$

Summarizing, the main conclusions that can be drawn from the present theoretical and experimental investigation are the following:

- The simplistic 4-parameter model presented here is able to reproduce the main features of FCG and threshold.
- The basic behavior of the threshold is characterized by two parameters,  $K_{max/th}$  and  $\Delta K_{th/int}$ , which can be obtained in principle from two tests performed on one single specimen.
- The cut compliance method is applicable to determine the crack closure SIF  $K_{op}$  even in the threshold range. It provides some additional information about crack closure.
- Significant crack closure (about  $0.3 \cdot K_{max}$  in the considered structural steel) is present even in the threshold regime
- Besides crack closure as measured by the CC-method, there are additional extrinsic shielding effects of nearly the same magnitude, which have similar effects on crack retardation and threshold as crack closure. These additional effects are expected to be less pronounced at the higher loads outside the threshold regime.
- The existence of "non-closure" shielding effects explains why opening loads determined by direct methods, are usually significantly smaller than the ones determined by indirect methods.

## References

- [1] Paris, P.C., "The fracture mechanics approach to fatigue," *Fatigue - an interdisciplinary approach*, J.J. Burke, N.L. Reed, V. Weiss, Eds., Syracuse University Press, NY, 1964, pp. 107-132.
- [2] Klesnil, M, Lucas, P., "Effect of Stress Cycle Asymmetry on Fatigue Crack Growth," *Materials Science and Engineering*, Vol. 9, 1972, pp. 231-240.
- [3] Wu, S., Mai, Y-W., Cotterell, B., "A Model of Fatigue Crack Growth Based on Dugdale Model and Damage Accumulation," *Int. J. Fracture*, Vol. 57, 1992, pp. 253-267.
- [4] Schindler, H.J. "Analytisches Modell zur Berechnung der Rissausbreitungs-geschwindigkeit unter Ermüdungsbeanspruchung," *Proc. 30. Tagung des DVM AK Bruchvorgänge*, DVM-Bericht 230, Deutscher Verband für Materialforschung und -prüfung, Berlin, 1998, 333-343 (in German).
- [5] Elber, W., "The significance of fatigue crack closure ," *Damage Tolerance in Aircraft Structures*, ASTM STP 486, American Society for Testing and Materials, Philadelphia, 1971, pp. 230-242.
- [6] Newman, J.C., "A crack closure model for predicting fatigue crack growth under aircraft spectrum loading," ASTM STP 748, American Society for Testing and Materials, Philadelphia, 1981, pp. 53-84.
- [7] Schijve, J., "Fatigue Crack Closure: Observations and Technical Significance," *Mechanics of Fatigue Crack Growth*, ASTM STP 982, J.C. Newman and W. Elber, Eds., ASTM, Philadelphia, 1988, pp. 5-34.
- [8] McClung, R.C., "The Influence of Applied Stress, Crack Length, and Stress Intensity Factor on Crack Closure," *Metallurgical Transactions A*, Vol. 22A, 1991, pp. 1559-1571.
- [9] James, M.N., "Some unresolved issues with fatigue crack closure-measurement, mechanism and interpretation problems," *Advances in Fracture Research*, ed. B.L. Karihaaloo, et al., Pergamon, Amsterdam, Vol. 5, 1997, pp. 2403-2413.
- [10] Louat, N., Sadananda, K., Duesbury, M., Vasudevan, A.K., "A theoretical Evaluation of Crack Closure," *Metall. Transactions A*, Vol. 24A, 1993, pp. 2225-2232.
- [11] Marci, G., "Determination of the Partitioning Point Dividing  $\Delta K$  into  $\Delta K_{\text{eff}}$ ," *Engineering Fracture Mechanics*, Vol. 53, 1995, pp 23-36.
- [12] Mc Evily, A.J., Ritchie, R.O., "Crack Closure and the Fatigue Crack Propagation Threshold as a Function of Load Ratio," *Fatigue and Fracture of Engineering Materials and Structures*, Vol. 21, 1998, pp. 847-855.

- [13] McClung, R.C., "Finite Element Analysis of Specimen Geometry Effects on Fatigue Crack Closure," *Fatigue and Fracture of Engineering Materials and Structures*, Vol. 17, 1994, pp. 861-872.
- [14] Rice, J.R., "Mechanics of Crack Tip Deformation and Extension by Fatigue," *ASTM STP 415*, American Society for Testing and Materials, Philadelphia, 1967, pp. 247-309.
- [15] Ritchie, R.O., and Yu, W., "Short crack effects in fatigue: a consequence of crack tip shielding," *The Metallurgical Society of AIME*, 1986, 167-189.
- [16] de Koning, A.U. and Liefing, G., "Analysis of Crack Opening Behaviour by Application of a Discretized Strip Yield Model," *ASTM STP 982*, J.C. Newman and W. Elber, Eds., ASTM, Philadelphia, 1988, pp. 437-458.
- [17] H. Döker, V. Bachmann, "Determination of Crack Opening Load by Use of Threshold Behaviour," *Mechanics of Fatigue Crack Growth*, ASTM STP 982, American Society for Testing and Materials, Philadelphia, 1988, pp. 274-259.
- [18] Schindler, H.J., "Charakterisierung und Abschätzung des Ermüdungsverhaltens im Bereich des Schwellenwerts," *DVM- Bericht 231*, Deutscher Verband für Materialforschung und -prüfung, Berlin, 1999, pp. 121-130 (in German).
- [19] Schmitt, R.A., Paris, P .C., "Threshold for Fatigue Crack Propagation ...," *ASTM STP 536*, American Society for Testing and Materials, Philadelphia, 1973, pp. 79-94.
- [20] Cheng, W., Finnie, I., "An Overview of the Crack Compliance Method For Residual Stress Measurement," *Proc. 4th Int Conf. On Residual Stress*, Baltimore,. Soc. Experimental Mechanics, 1994, pp. 449-458.
- [21] Schindler, H.J., Cheng, W., Finnie, I., "Experimental Determination of Stress Intensity Factors due to Residual Stresses," *Experimental Mechanics*, Vol. 37, No. 3, 1997, pp. 272-279.
- [22] Schindler, H.J., "Experimental Determination of Crack Closure by the Cut Compliance Technique ," to be published in: *Advances in Fatigue Crack Closure Measurement and Analysis*, ASTM STP 1343, R.C. McClung and J.C. Newman, Jr., Eds., American Society for Testing and Materials, West Conshohocken, 1999.
- [23] Schindler, H.J., Finnie, I., "Determination of Residual Stresses and the Resulting Stress Intensity Factors in the Ligament of Pre-cracked Components," *Advances in Fracture Research*, B.L. Karihaaloo, et al., eds.(Proceedings of 9th Int. Conf. on Fracture), Sydney, Pergamon, Amsterdam, Vol. 1, 1997, pp. 523-530.
- [24] Bertschinger, P, Schindler, H.J., Soyka, G., "Experimentelle Ermittlung der Risschliessung an Baustahl und Schweisseisen im Bereich des Schwellenwerts," *DVM- Bericht 231*, Deutscher Verband für Materialforschung und -prüfung, Berlin, 1999, pp. 153-161 (in German).